CHAPTER IV

THERMAL, CRYSTALLIZATION, AND MECHANICAL CHARACTERISTICS OF POLY(D,L-LACTIDE) BLEND FIBERS CONTAINING ANTIBACTERIAL ELEMENTS FOR BIOMEDICAL APPLICATIONS BY USING MELT SPINNING TECHNIQUE

Saran Suntarin, *Pitt Supaphol*

The Petroleum and Petrochemical College, Chulalongkorn University, Bangkok, Thailand

4.1 Abstract

Poly(d,l-lactide) (PDLLA) was improved the properties by blending with Poly[(*R*)-3-hydroxybutyrate-*co*-(*R*)-3-hydroxyvalerate] (PHBV) and poly(ethylene glycol) (PEG1000), which were also developed in antimicrobial efficiency by adding silver nitrate ($AgNO_3$) and they were spun into fiber by melt-spinning technique. DSC data showed that the PDLLA/PHBV blends presented two distinct glass transitions (T_g) and they have not changed position when comparing with polymer blends indicating that these blends were immiscible in all compositions. The PDLLA/PHBV/PEG1000 showed the miscibility between PEG1000 and PDLLA/PHBV as evidenced by the decreasing in T_g as compared to the neat PDLLA/PHBV. For TGA data, Neat PDLLA was more thermally stable than neat PHBV and TGA curves comprising of those neat components showed two degradation steps. The addition of PEG1000 caused a shift of the onset temperature to a lower temperature but the thermal degradation temperature (T_d) of later thermal weight-loss stage shifted to a higher temperature. The addition of PHBV and PEG1000 caused an increase in elongation at break from 3.7% for PDLLA to 413.8% for PDLLA/PHBV/PEG1000. The antibacterial results showed that it can constrain E. coli and S. aureus and can release silver ion for more than 18 days.

Keywords: Poly(d,l-lactide), PDLLA, Poly[(*R*)-3-hydroxybutyrate-*co*-(*R*)-3-hydroxyvalerate], PHBV, poly(ethylene glycol), PEG, silver nanoparticles

4.2 Introduction

In present, fibers have an important role in daily life of human because it can be used in many applications such as clothing, composites, separation membranes and biomedicine. From all of the applications, biomedical application has the most impact. It has received significant attention in last few years which strongly contributed to the development.

Fibers for biomedical applications represented a new class of material as drug delivery systems, wound dressing, breathing mask and absorbable suture are usually made from biodegradable polymers such as poly(lactide) (PLA), poly(3-hydroxybutyrate) (PHB) and Poly[(*R*)-3-hydroxybutyrate-*co*-(*R*)-3-hydroxyvalerate] (PHBV) because they produces a biodegradable, biocompatible and non-toxic thermoplastic polyester with excellent functional properties comparable to many petroleum-based plastics. Further advantages are that they can be synthesized from renewable resources so it represents an interesting way to replace petroleum based polymer, especially from the viewpoint of environmental protection. But the all of above polymers have some disadvantage such as in PLA, it has glass transition temperatures above room temperature, rendering is hard and brittle but it has high tensile strength (M.E. Broz *et al.*, 2006). In PHB, it is poor in mechanical properties and it is brittle which may limit their applications in situations that require high tensile strength (Y. Furuhashi *et al.*, 2004). In PHBV, although it has poor mechanical properties but it is flexible. Thus, the mechanical properties of these polymers should be improved before using in some biomedical applications such as suture which require high tensile strength and high flexibility. The suitable technique for fitting this requirement is the blending technique which is used to prepare a novel blend polymer of two or more polymers in required properties without having to synthesize a totally new material. And to further improve their mechanical property, plasticizer is also added. The plasticizer used is poly(ethylene glycol) (PEG) because PEG is good in biocompatibility and blood compatibility. Moreover, it can act as a stabilizer and reducing agent (C. Luo *et al.*, 2005) which is suitable to use in synthesis of metal nanoparticle in a polymer matrix. There are many researchers that have done studies on PDLLA/PEG (S. Muriel *et al.*, 2006), PHBV/PEG (D.F. Parra *et al.*, 2006) and PLA/PHBV/PEG (S. Wang *et al.*, 2008)

And the other development of these blending fibers to be used for a wider biomedical application is the addition of antimicrobial efficiency into blended fibers to prevent micro-organisms growth (Xiaoyi Xu *et al.*, 2006, Fahmina Zafar *et al.*, 2007), by using a powerful antimicrobial agent as silver, titanium, zinc compound in nanopractical size.

In the method to form fibers for biomedical applications, electrospinning technology has received much interest because this method is capable to produce fibers with high specific surface area. The fibers are collected as non-woven with a diameter ranging from 10 nm to 500 nm and small porous web which is suitable for biomedical such as tissue-engineering scaffolds (Xiaoyi Xu *et al.*, 2006). But electrospinning method has some disadvantages. It is that this method produces non-woven which inhibits the use of special process to improve mechanical properties of fibers (such as drawing). Also the poor mechanical properties of the fiber will limit the use of various biomedical applications such as suture or dental floss because suture and dental floss are always monofilament fiber and require high tensile strength. For solving this problem, melt spinning is alternative method to produce fibers which have high mechanical properties.

Melt spinning method can produce monofilament fibers with a micrometer of diameter and can produce high tensile strength fiber depending on process or materials such as two different speed of roll for drawing fibers and characteristic of each polymer.

The purpose of this work is to produce biodegradable blends as PDLLA/PHBV/PEG1000 containing silver nanoparticles for antibacterial function in biomedical applications by using melt spinning method.

4.3 Experimental

4.3.1 Materials

Poly(d,l-lactide) 4042D (PDLLA) (NatureWorks®) (Mw = 74,000 g/mol) consisting of 92% L-lactide and 8% D-lactide units were supplied from Asst. Prof. Sommai Pivsa-Art, Poly(3-hydroxybutyrate-co-3-hydroxyvalerate) (Mw = 680,000 g/mol) was purchased from Sigma Aldrich, USA with HV content of 5 mol% of PHBV, Poly(ethylene glycol) (Mw = 1,000) was purchased from Fluka, Switzerland and silver nitrate ($AgNO_3$;99.998% purity) was purchased from Fisher Scientific, USA. All chemicals were of analytical grade and used without further purification.

4.3.2 Polymer Blend Preparation

The dried PDLLA and PHBV was dissolved in hot chloroform at 50°C for 2 hours to produce PDLLA/PHBV pre-blends of 10%, 20%, 30%, 40%, and 50% w/w of PHBV.

In the case of PDLLA/PHBV/PEG1000, The suitable composition of PDLLA/PHBV was blended with PEG1000 at 10%, 20%, 30% and 40% w/w by dissolving in hot chloroform solvent at 50°C for 2 hours.

And in the case of PDLLA/PHBV/PEG1000/silver nanoparticles, the suitable PDLLA/PHBV/PEG1000 was blended with silver nitrate at 0.2%, 0.3% and 0.4% w/w after dissolving $AgNO_3$ in 50/50 chloroform-to-dimethylformamide ratio and then stirred for 24 hours to produce silver nanoparticles.

All of polymer solutions were precipitated by dropping *n*-hexane into polymer blend solution and then blended samples were dried under vacuum at 50°C for 48 hours and were stored under vacuum in desiccators until spinning.

4.3.3 Melt Spinning Process

The PDLLA/PHBV fibers were spun at 180°C, 1.5 mm/min of piston velocity and 20 m min^{-1} of take up speed by using a melt spinning machine from Venture & Consultancy Bradford Ltd. The minimal dead volume within the system enable sample sizes of as small as 10 g to be processed satisfactorily. The water cooling bath is maintained at a temperature of 30°C, while the vertical distance of air gap between a 1 mm single-hole spinneret and the surface of the water cooling bath is kept constant at 2 cm.

The PDLLA/PHBV/PEG1000 and PDLLA/PHBV/PEG1000/silver nanoparticle were spun by using the same melt spinning machine and same conditions as above with spinning temperature of 170°C.

4.3.4 Characterizations

4.3.3.1 Thermal Stability

The decomposition temperatures (T_d) for PDLLA and their blends were measured with a Mettler Toledo Thermogravimetric Analyzer/ Differential Scanning Calorimeter (TGA/DSC) within the temperature range from 25°C to 500°C. The heating rate during thermal scanning is fixed at 10 °C min^{-1}.

4.3.3.2 Miscibility, Crystallization and Melting Behaviour of Polymer Blends

Differential Scanning Calorimeter (DSC) is used to record the non-isothermal cold and melt-crystallization exotherms as well as the subsequent melting endotherms for PDLLA and their blends. The experiments started with heating PDLLA and their blends from 25°C to a fusion temperature of 200°C at a rate of 20°C min^{-1} for a melt-annealing period of 10 min to reset previous thermal histories, after which the samples were taken out and immediately quenched in liquid nitrogen to attain the completely amorphous state of the samples. To observe the non-isothermal cold-crystallization and subsequent melting behavior, each sample was reheated again with DSC from -60 to 200°C at a rate of 10°C min^{-1}.

4.3.3.3 Mechanical Properties

The mechanical properties are observed by the tensile testing at room temperature according to ASTM D3822-07 by using an Instron universal testing machine. The tests were carried out at cross-head speed 60 mm min^{-1} and 25 mm of gauge length. The results obtained were averaged over ten samples for each condition. The reports showed the physical break stress, initial E-modulus and elongation at break.

4.3.3.4 Morphological Property

The surface topography and silver nanoparticles distribution on surface of fibers were investigated by JEOL JSM-5200 Scanning Electron Microscopy (SEM).

4.3.3.5 Effect of Reduction Time on Concentration and Size of Silver Nanoparticles

UV-visible absorption spectra were used to observe the reduction of the silver ions to metallic silver nuclei or silver nanoparticles. The intensity of the surface plasmon resonance absorption at 416 nm was observed with time. Moreover, TEM images of the silver nanoparticles after the preparation of the solution was observed their average diameter and their size distribution in polymer blend mixture.

4.3.3.6 Silver Ion Release

The fibers containing silver nanoparticles were cut into many 1.0 cm in pieces, which weighed approximately 0.4 g. The in vitro release of silver ions were carried out in 5 mL of 0.02 mol L^{-1} phosphate buffered saline (PBS, pH= 7.4). The samples are incubated at 37°C under oscillation of 50 round min^{-1}. The silver ions concentration in the solution released is measured every 24 hours over 18-day test period by an atomic absorption spectrometer (AAs).

4.3.3.7 The Agar Diffusion Test

This method is used to observe antibacterial efficiency that will be performed in nutrient broth medium solid agar Petri dish. Starting with inoculating E. coli and S. aureus bacteria into a growth medium. Approximately 10^8 CFU of each microorganism will be spread on agar plates. After that, the fibers containing silver nanoparticles will be cut into many 1.0 cm in pieces and then placed on E. coli and S. aureus cultured agar plates, which will be incubated for 24 h at $37^{o}C$. The zone of inhibition will be measured for clear zone.

4.4 Results and Discussion

4.4.1 PDLLA/PHBV blends

4.4.1.1 Effect of PHBV on the Thermal and Mechanical Property of PDLLA/PHBV

a) Thermal Behaviour of PDLLA/PHBV

The thermal behaviour of neat PDLLA, neat PHBV and their blends was determined by DSC that can be used to observe glass transition temperature (T_g), cold-crystallization peak temperature (T_{cc}) and melting temperature (T_m). Figure 4.1 and Table 4.1 show DSC data for quenched PDLLA, quenched PHBV and their blends in 10%, 20%, 30%, 40%, and 50% w/w of PHBV.

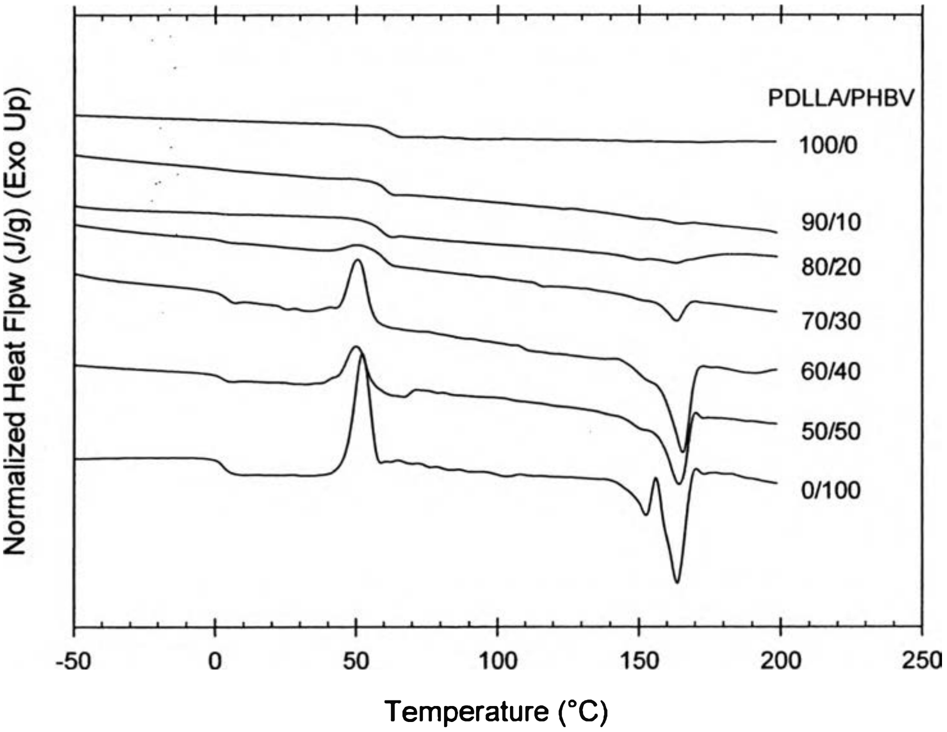

Figure 4.1 DSC thermograms of quenched PDLLA/PHBV blends.

In the case of PDLLA, when it was mixed with PHBV, T_g of PDLLA could be only observed in neat PDLLA, because in the other composition T_g of PDLLA was overloaded by the T_{cc} peak of PHBV. In 80% and 90% of PDLLA, a small T_g of PDLLA was observed because those compositions had small amount of PHBV so it has only received small affect of T_{cc} peak of PHBV. As for neat PDLLA, it has very poor crystallization because it shows a very small melting endotherm in comparison to thermodynamical melting enthalpy of 94 J g^{-1} for fully crystalline PLA (Tsuji *et al.*, 1996).

In the case of PHBV, T_g, T_{cc} and T_m were observed around 0°C, 50°C and 165°C, respectively, which were no variation in all compositions when comparing to pure polymers. According to Penning and Manley, the crystallization of each blend compositions shows a phase separation process it means the each polymer partially segregate from the mixture to form a pure phase of that polymer (Penning *et al.*, 1996).

Variations on the cold-crystallization and melting enthalpies for the polymer blends are shown in Table 4.1. They show that when the content of PHBV polymer in the polymer blends was reduced, its cold-crystallization and melting enthalpy also decreases and when the PHBV polymer composition was very small, they almost disappeared (Iannace *et al.,* 1994). As for the cold-crystallization and melting enthalpy neat PHBV, it show this value is lower when comparing with polymer blend as a results from PDLLA polymer in polymer blend can also act as nucleating agent to increase the crystallization of these polymer blends.

From all data, PDLLA/PHBV is indicated to be immiscible in all compositions.

Table 4.1 Glass transition, cold-crystallization and melting temperature and their enthalpies of neat PDLLA, neat PHBV and their blends.

Polymer blends (PLA/PHBV)	T_g (°C)		T_m (°C)	ΔH_m (J g^{-1})	T_c (°C)	ΔH_c (J g^{-1})
	PLA	PHBV				
100/10	61.34	-	-	-	-	-
90/10	60.34	-	-	-	-	-
80/20	57.72	-	-	-	-	-
70/30	-	-0.22	163.61	-37.03	51.76	37.25
60/40	-	1.22	165.81	-233.20	50.64	126.30
50/50	-	-0.48	164.57	-274.51	50.13	144.48
0/100	-	-0.56	164.02	-142.65	52.36	98.82

b) Thermal Stability of PDLLA/PHBV

Thermal stability is important during melt processing of aliphatic polyesters because their melting and thermal decomposition ranges are in close proximity. TGA is the most popular method for characterizing the thermal stability of polymers. TGA curves in Figure 4.2 shows thermal degradation temperatures (T_d) step of neat PDLLA and neat PHBV which were at 323.04°C and 264.19°C, respectively and also show that PDLLA degraded at a higher and a broader temperature range than PHBV. In the case of their blends, the curves are comprised between those for pure components, and all of them show more than one degradation step. The results reveal that neat PDLLA, neat PHBV and their blends were thermal stable within the temperature used in spinning processing (180°C). Moreover, they also reveal and support the DSC data that their blends are immiscible in all composition.

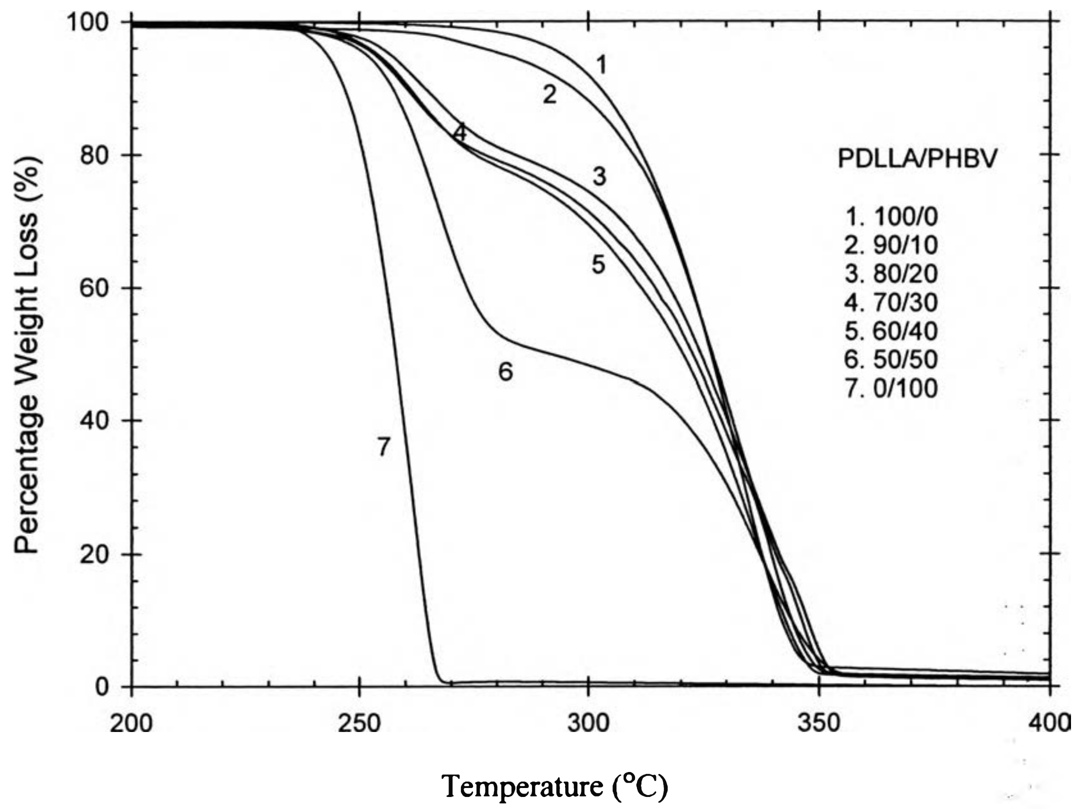

Figure 4.2 Thermogravimetric curves for PDLLA/PHBV blends of different compositions.

c) Mechanical Property of PDLLA/PHBV

Mechanical properties were compared and used to select the suitable ratio of polymer blends to spin fiber containing silver nanoparticles. Table 4.2 shows breaking tenacity, initial modulus, and elongation at break of various rations of PDLLA/PHBV blend fibers by using D 3822-07 standard test method. (The value neat PHBV fiber is not shown because it cannot be spun in these conditions) Moreover, the tensile behaviour of neat PDLLA and PHBV blends is shown in Figures 4.3.

Table 4.2 shows that the addition of PHBV does not affect the breaking tenacity but affects initial modulus and elongation at break, which has improved at these properties. The addition of 50% w/w of PHBV into PDLLA increase the elongation at break of the fiber by about 300% compared to pure PDLLA and the elongation at break is insensitive to composition from 10%, 20% and 30% w/w of PHBV that shows a linear increase.

Table 4.2 Mechanical properties of PDLLA/PHBV blends.

Blend Composition	Breaking Tenacity (g/den)	Elongation (mm)	Initial Modulus (g/den)
PDLLA	0.542±0.019	0.914±0.063	25.671±1.154
90 PDLLA/10PHBV	0.516±0.031	1.046±0.182	21.501±1.779
80 PDLLA/20PHBV	0.405±0.042	1.142±0.218	20.753±1.142
70 PDLLA/30PHBV	0.454±0.02	5.797±1.507	24.126±0.944
60 PDLLA/40PHBV	0.446±0.027	47.239±3.618	25.328±0.728
50 PDLLA/50PHBV	0.499±0.055	84.086±10.688	32.808±2.829

Stress-elongation curves of tensile behaviour as shown in figure 4.3 shows that the addition of PHBV into neat PDLLA can change the tensile behaviour of neat PDLLA. It means that the brittle-fracture of neat PDLLA can convert into ductile-fracture of the PDLLA/PHBV blends. Neat PDLLA shows a failure yield point immediately upon the tensile load which contrasts with other blends. The other blends show a stable neck which can increase the elongation continuously.

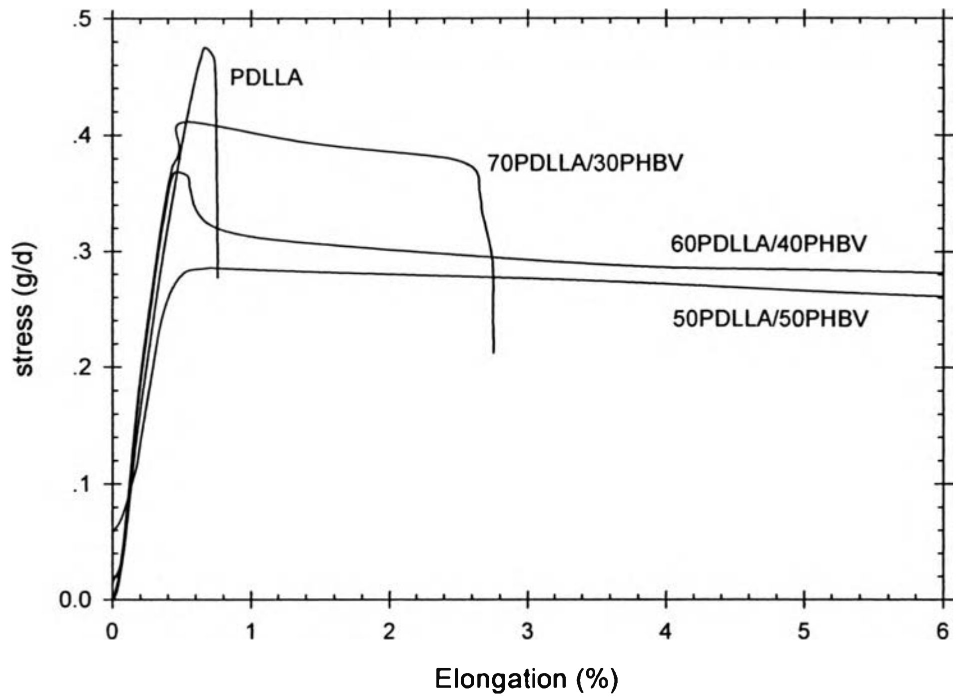

Figure 4.3 Tensile stress-extension curves of PDLLA/PHBV blends.

4.4.2 PDLLA/PHBV/PEG1000 blends

4.4.2.1 Effect of PEG1000 on the Thermal and Mechanical Property of PDLLA/PHBV/PEG1000

a) Thermal Behaviour of PDLLA/PHBV/PEG1000

- Miscibility of PDLLA/PHBV/PEG1000 Blends

There are many research of PDLLA or PHBV plasticized with PEG. They demonstrated that when the molecular weight of PEG is reduced, it will increase efficiency of plasticization. And the low molecular weight of the plasticizer also increases miscibility (Kulinski *et al.*, 2005), so in this work, PEG with low molecular weight of only 1000 is chosen. Moreover, PEG can also act as a stabilizer and reducing agent (C. Luo *et al.*, 2005) during synthesis of metal nanoparticle in a polymer matrix.

From the results of mechanical property of PDLLA/PHBV blends, they show that 50PDLLA/50PHBV has the highest elongation within the studied composition range so this blend was chosen to be blend with PEG1000. Figure 4.4 displays the DSC cold-crystallization and subsequent melting thermograms for quenched PDLLA/PHBV, PEG1000, and their blends recorded in various composition of PEG1000. It is apparent that T_g value of PHBV is still observed in each thermogram but it is located between neat PHBV and PEG1000 components (i.e., T_g, PHBV = -1 °C and T_g, PEG1000 = -81 °C) decreased with an increasing PEG1000 content as show in Figure 4.4 and 4.5. The results clearly suggest that PHBV and PEG1000 were fully miscible in the amorphous phase at all blend compositions. In the case of PDLLA, it is still received the affect of crystallization peak of PHBV overloaded the T_g of PDLLA so it cannot observe the affect of addition PEG1000 in PDLLA part.

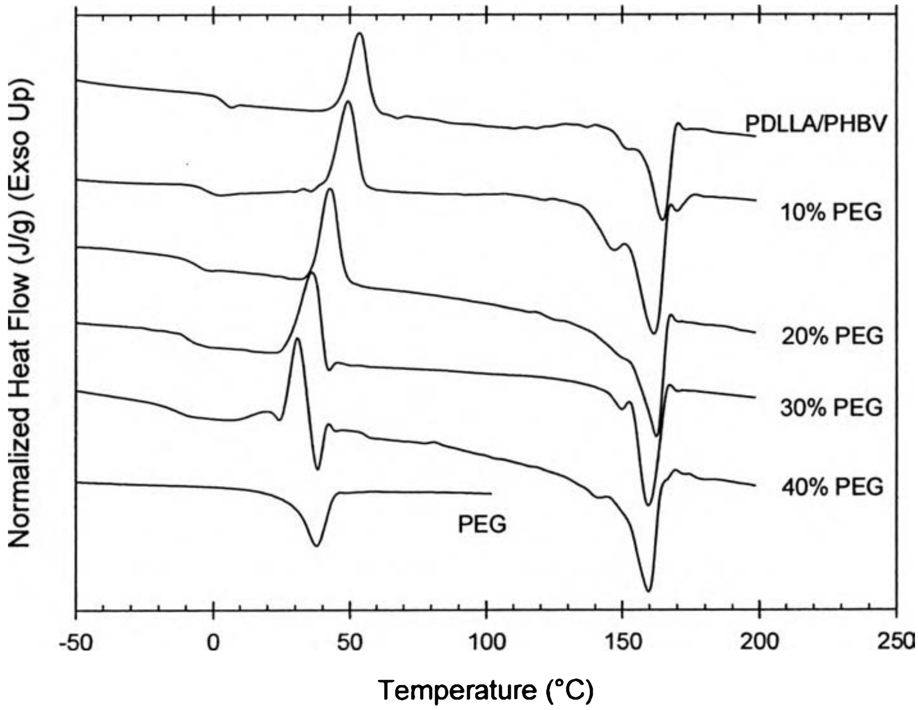

Figure 4.4 DSC Thermograms of quenched PDLLA/PHBV/PEG1000 blends in various PEG1000 component.

A number of empirical models were use to predict the location of T_g between the T_g of two neat polymer indicating miscible blends; some of these are the Gordon–Taylor (Gordon *et al.*, 1952), Fox (Fox *et al.*, 1956), Couchman–Karasz (Couchman *et al.*, 1978), and Utracki (Utracki *et al.*, 1985) equations. These equations predict a monotonic dependence of the T_g value on the blend composition without any cusp in the predicted curve. Among these, the Gordon–Taylor equation, which reads

$$T_g = \frac{w_1 T_{g1} + k w_2 T_{g2}}{w_1 + k w_2}$$

where w_1 and w_2 are the weight fractions (in the amorphous phase) of components 1 and 2, respectively, T_{g1} and T_{g2} are the T_g values of the pure components 1 and 2, respectively, and k is an adjustable parameter. The compositional dependence of T_g for the PDLLA/PHBV/PEG1000 blends was also well predicted by the Gordon–Taylor equation as show in Figure 4.5 with the k parameter being about 0.525.

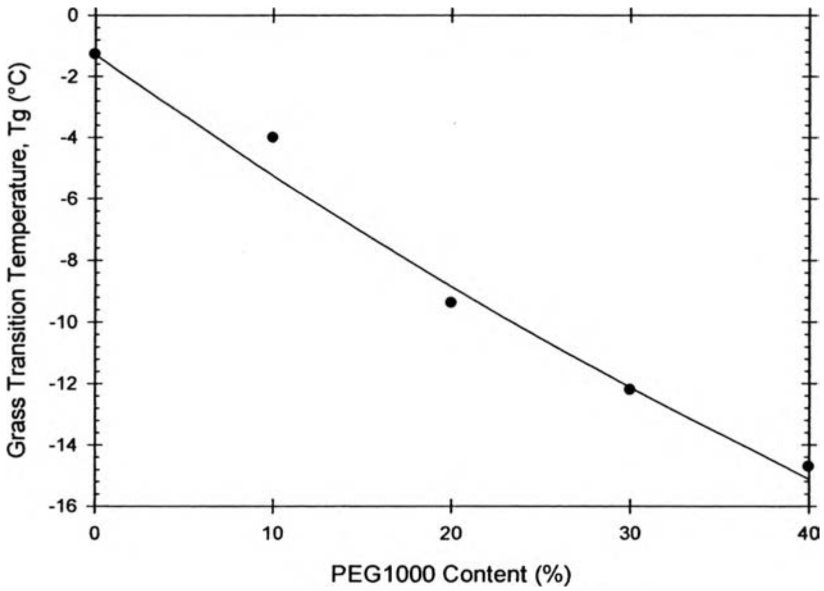

Figure 4.5 Observed glass transition temperature (T_g) for quenched PDLLA/PHBV/PEG1000 blends in various PEG1000 contents. The solid line is the predicted T_g curve according to the Gordon–Taylor equation, with the fitting parameter k of 0.525.

- Crystallization Behaviour

According to Figure 4.4 the cold-crystallization peak temperature (T_{cc}) for PHBV was observed around 52.9 °C, and this value will be decreased hypothetically linearly from around 52.9 to 30.7 °C with increasing PEG1000 content. The observed T_{cc} values for PDLLA/PHBV/PEG1000 blends as well as for the neat components were plotted against the PEG1000 composition in Figure 4.6. The results suggested that both PHBV and PEG1000 components crystallized simultaneously and the homogeneous and the addition of the more crystallizable PEG1000 to PHBV helped promote the crystallization of the blends (i.e. crystallization temperature decreasing). The selection of short chain PEG1000 indicates a higher mobility of PHBV macromolecules. This enhancement of the PHBV molecular mobility is claimed to be the major factor acting on the crystallization kinetic of this polymer (Pillin *et al.*, 2006).

Moreover, Table 4.3 presented more details about thermal analysis parameters of this blends including the degree of crystallinity. It was calculated using the following equation (Liu *et al.*, 1997):

$$X_c (\%) = (\Delta H_m + \Delta H_c) \text{ x } 100 / (\Delta H^o_m \text{ x } X_{PHBV})$$

where ΔH_m is the enthalpies (J/g) of fusion of melt PHBV and ΔH_m is enthalpies (J/g) of fusion of crystallization of the blends, and 114 J/g is the enthalpy of 100% crystalline PHBV (Bin Fei *et al.*, 2003) X_{PHBV} is the percentage of the PHBV content.

The crystallinity of PHBV phase increased obviously with increasing PEG1000 content because PEG1000 acts as a plasticizer and had a positive influence on the chain mobility of PHBV and a better packing of the chains and thus improved the crystallization capacity.

But in the addition of 40% PEG1000, the DSC data shows that the observed T_{cc} values for this blend composition show some of phase-separate in crystallized part as evidenced by the occurring of melting peak temperature (T_m) of PEG1000 as show in Figure 4.4. It can assume that the large enhancement of the crystallinity of PHBV is the major cause for the phase separation at 40% of PEG1000 (Pillin *et al.*, 2006).

Table 4.3 Thermal analysis parameters of PDLLA/PHBV/PEG1000 blends

Polymer blends (PDLLA/PHBV/PEG1000)	T_m (°C)	ΔH_m (J g^{-1})	ΔH_c (J g^{-1})	C_{PHBV} (%)
50/50/0	166.619	-36.3	27.74	15.01
10% PEG	161.184	-58.96	28.98	57.86
20% PEG	160.971	-62	29.08	69.38
30% PEG	158.386	-63.67	29.04	78.99

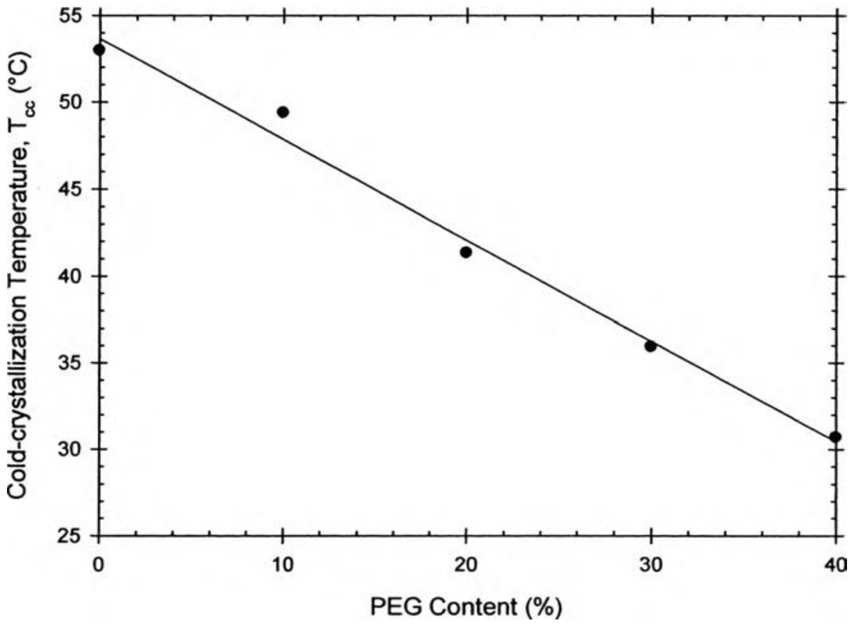

Figure 4.6 Observed cold-crystallization temperatures (T_{cc}) for quenched PLA/PHBV/PEG1000 blends in various PEG1000 content.

- Melt Behaviour

The subsequent melting thermograms for PHBV, PEG1000 and their blends in PDLLA/PHBV/PEG1000 blends after cold-crystallization are shown in Figure 4.4. The thermograms for both PHBV and PEG1000 samples exhibited single melting endothermic peaks, with the observed T_m values being observed about 166.6 °C and 38 °C, respectively. Figure 4.7 shows a plot of the observed T_m values against the PEG1000 content in the blends. It shows that the observed T_m value of the major component in the blends decreased with increasing amount of the minor component.

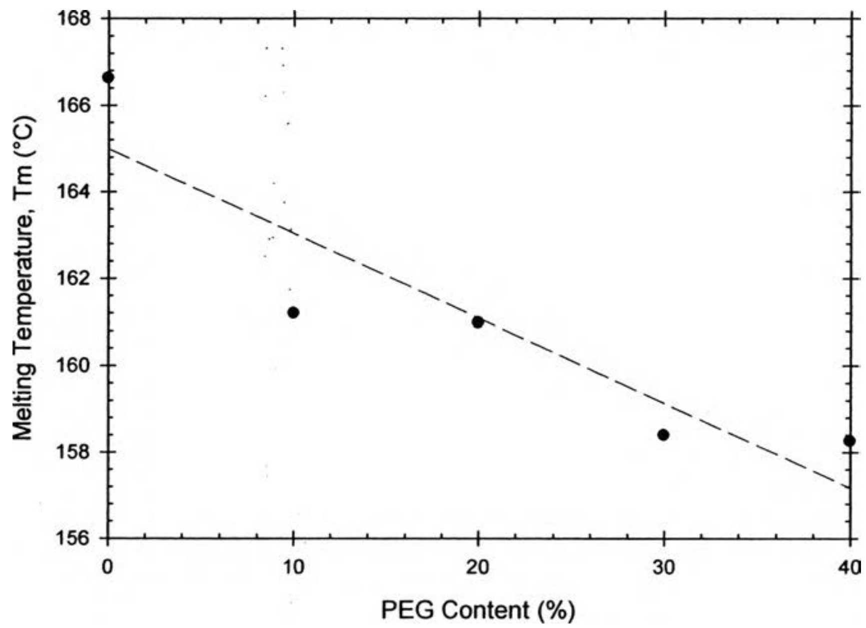

Figure 4.7 Observed melting temperature (T_m) for PDLLA/PHBV/PEG1000 blends in various PEG1000 content.

b) Thermal Stability of PDLLA/PHBV/PEG1000

TGA curves are shown in Figure 4.8 which shows that the addition of PEG1000 cause a slightly shift of the degradation temperature (T_d) of 50PLA/50PHBV/PEG1000 blends to a lower temperature, but T_d of later thermal weight-loss stage shifted to a higher temperature.

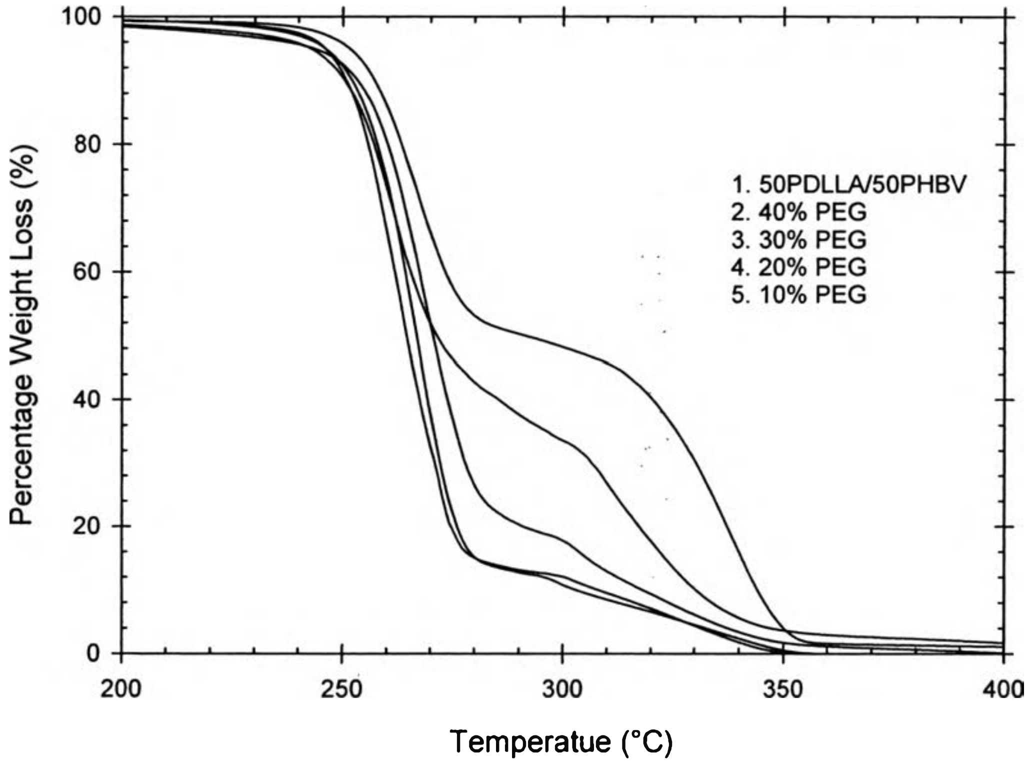

Figure 4.8 Thermogravimetric curves for PDLLA/PHBV/PEG1000 blends in various PEG1000 content.

c) Mechanical Property of PDLLA/PHBV/PEG1000

PEG1000 which acts as plasticizer is blended with PDLLA/PHBV blend to improve their mechanical property before spinning into fibers containing silver nanoparticles. The addition of PEG1000 decreased melt-viscosity of PDLLA/PHBV blend so a spinning temperature of 180°C made these blends difficult to spin so the temperature used in this blend is changed to 170 °C. This temperature is also used to spin the fibers containing silver nanoparticles.

Table 4.4 shows the breaking tenacity, elongation and initial modulus of 50PDLLA/50PHBV and their blends. The results indicate that breaking tenacity and initial modulus were significantly reduced from 0.51 g/d to 0.27 g/d and from 21.6 g/d to 9.9, respectively caused by the addition of PEG1000, but the elongation at break increased from 90.1 mm to 103.5 mm. From all of these results, the weight ratio as 50PDLLA/50PHBV/30% PEG1000 is the most suitable composition to spin fibers containing silver nanoparticles because it showed some characterstics of flexible materials.

Table 4.4 Mechanical properties of PDLLA/PHBV/PEG1000 blends.

Blend Composition	Breaking Tenacity (g/den)	Elongation (mm)	Initial Modulus (g/den)
50PDLLA/50PHBV	0.510±0.035	90.058±0.737	21.671±1.054
10% PEG	0.324±0.028	88.249±4.443	20.101±1.279
20% PEG	0.317±0.038	95.059±3.958	17.753±1.242
30% PEG	0.271± 0.021	103.445±3.662	9.986±9.986

4.4.3 PDLLA/PHBV/PEG1000/Silver Nanoparticles

4.4.3.1 Effect of Silver Nanoparticles on the Thermal and Mechanical Property of PDLLA/PHBV/PEG1000/Silver Nanoparticle

a) Thermal Behaviour of PLA/PHBV/PEG1000/Silver Nanoparticle

To develop the PDLLA/PHBV/PEG1000 blend fibers for using in much wider biomedical applications, the addition of antimicrobial function into blending fibers to sustain micro-organisms growth was an alternative. The antimicrobial additive that has received interest is silver nanoparticles.

DSC data of PDLLA/PHBV/PEG1000/silver nanoparticle is shown in Figure 4.9. It showed that the addition of silver nanoparticles does not influence the T_g and T_m of PHBV in PDLLA/PHBV/PEG1000/silver nanoparticles blend. Nevertheless, the cold-crystallization temperature (T_{cc}) of PHBV slightly increased when silver nanoparticles are added as show in Figure 4.10. It is the results from the obstruction of silver nanoparticles to crystallization of polymer blends.

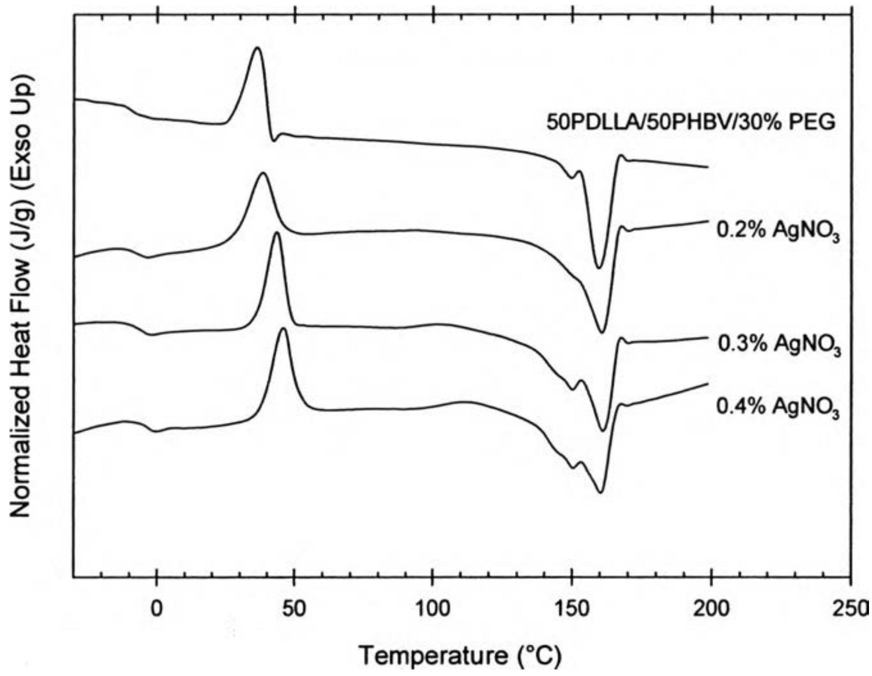

Figure 4.9 DSC Thermograms of quenched PDLLA/PHBV/PEG1000/silver nanoparticles blends in various silver nanoparticles component.

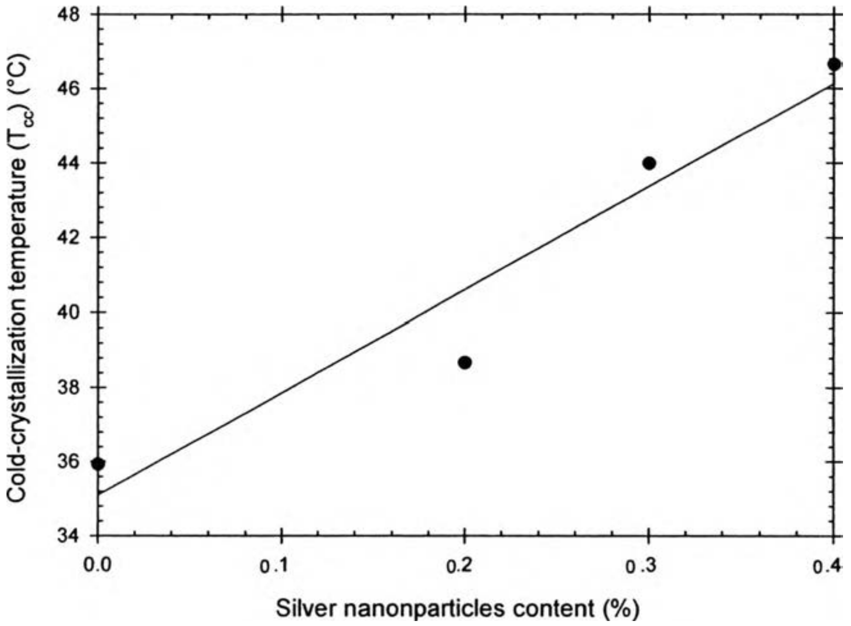

Figure 4.10 Observed cold-crystallization temperature (T_{cc}) for quenched PDLLA/PHBV/PEG1000/ silver nanoparticles blends in various silver nanoparticles component

b) PDLLA/PHBV/PEG1000/Silver Nanoparticles

TGA curves are shown in Figure 4.11 which shows that the addition of silver nanoparticles causes an obvious shift of the degradation temperature (T_d) of PDLLA/PHBV/PEG1000/silver nanoparticles blends to a higher temperature. Moreover, T_d of later thermal weight-loss stage also shifted to a higher temperature.

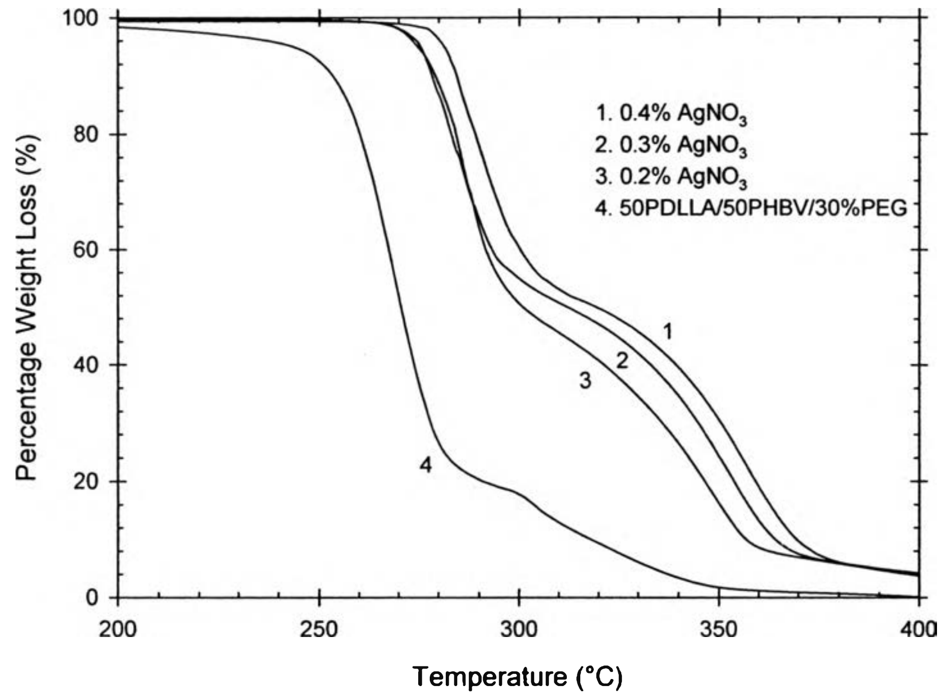

Figure 4.11 Thermogravimetric curves for PDLLA/PHBV/PEG1000/silver nanoparticles blends in various silver nanoparticles content.

c) Mechanical Property of PDLLA/PHBV/PEG1000/
Silver Nanoparticles

The mechanical properties of PDLLA/PHBV/PEG1000 with various amount of silver nitrate were shown in Table 4.5. Breaking tenacity, elongation and initial modulus decrease when the content of silver nanoparticles was increased. The elongation at break obviously decreases with the 0.3 wt % of silver nitrate. All of results are explained by a lack of cohesion between the phases which have silver nanoparticles.

Table 4.5 Mechanical properties of PDLLA/PHBV/PEG1000/silver nanoparticles blends

Blend Composition	Breaking Tenacity (g/den)	Elongation (mm)	Initial Modulus (g/den)
50PDLLA/50PHBV/PEG1000	0.271±0.021	103.445±3.662	9.986±9.986
0.2 % Silver nitrate	0.178±0.007	75.763±8.572	18.215±1.279
0.3 % Silver nitrate	0.149±0.001	33.613±3.936	10.371±0.711
0.4 % Silver nitrate	0.137±0.005	1.254±0.452	8.748±1.422

4.4.3 Antibaterial Test in PDLLA/PHBV/PEG1000/Silver Nanoparticle

4.4.3.1 Effect of Reduction Time on Concentration and Size of Silver Nanoparticles in PDLLA/PHBV/PEG1000 Solution.

In this work, PDLLA/PHBV/PEG1000 solution containing silver nanoparticles was prepared by reducing silver ion using PEG1000 as reducing and stabilizer agent. Figure 4.12 shows the intensity of surface plasmon resonance absorption of 50PDLLA/50PHBV/0.4 wt. % silver nitrate solution without PEG1000. This test was done for confirming the efficiency of PEG1000 to generate silver nanoparticle by comparing with Figure 4.13 that shows the changes in the UV-visible absorption spectra of a 50PDLLA/50PHBV and 30% of PEG1000 containing 0.4 wt. % silver nitrate solution. The results indicate that PEG1000 has an efficiency to generate silver nanoparticle from silver ion.

In the study of the reduction of silver ion depending on time, it also shows that a dark yellow coloration could be observed with the naked eye after a certain initial time period, confirming the reduction of the silver ion and the subsequent formation of metallic Ag nuclei. These results are also confirmed by observation in Figure 4.13 that shows the intensity of the surface plasmon resonance absorption at 416 nm was increased with time. From the UV results, the position of maximum absorbance was not shifted to higher wavelength, indicating that the average size of the Ag nanoparticles was not increased with increasing time (Sondi *et al.*, 2004).

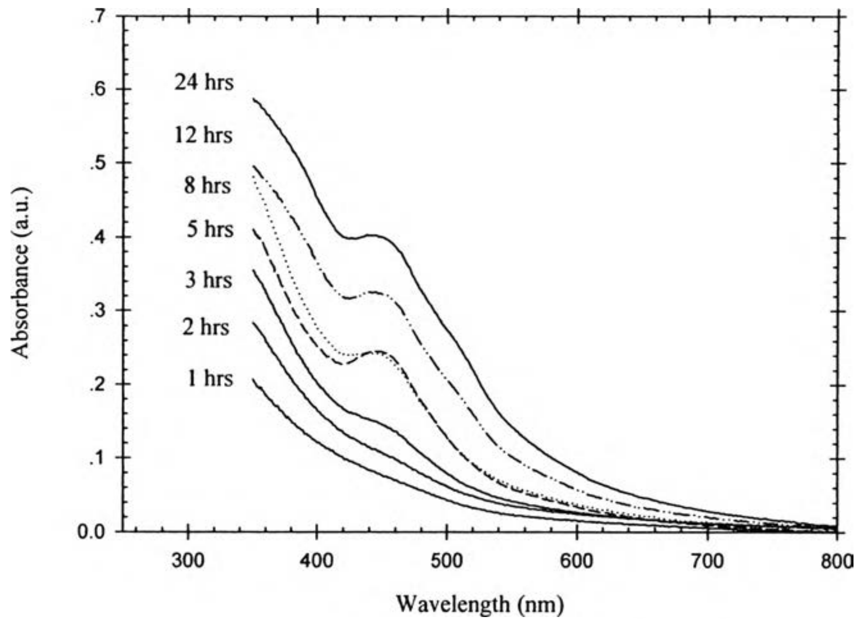

Figure 4.12 Changing in UV-visible absorption spectra of PDLLA/PHBV/0.4 wt. % silver nitrate without PEG1000.

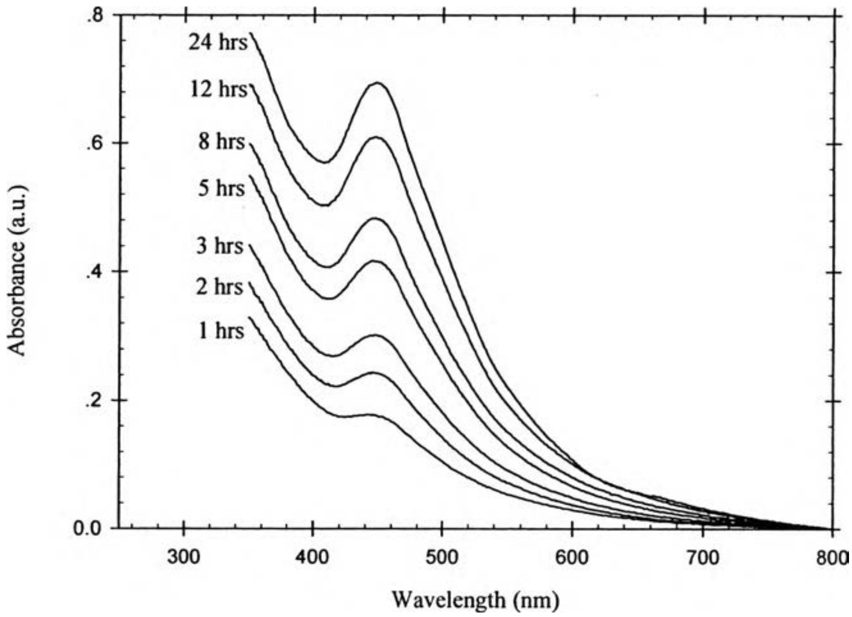

Figure 4.13 Changing in UV-visible absorption spectra of PDLLA/PHBV/PEG1000 containing 0.4 wt. % silver nitrate.

4.4.3.2 Morphological Property of Fiber Containing Silver Nanoparticles

The surface topography and silver nanoparticles distribution on surface of fibers were investigated by scanning electron microscopy (SEM). Figure 4.14 and Figure 4.15 demonstrates SEM images of PDLLA/PHBV/PEG1000 fiber without and containing silver nanoparticle when adding silver nitrate in 0.2, 0.3, 0.4 wt.% of fiber. SEM at magnitude of 750 times (Figure 4.14) shows that the fiber diameters are dramatically decreased when silver nitrate was added because the addition of silver nitrate decrease the melt-viscosity of this blend affecting the diameter of fiber and Figure 4.15 at higher magnitude shows the distribution of silver nanoparticles in fibers. They show that the silver nanoparticles were found to agglomerate with increase silver nanoparticles content.

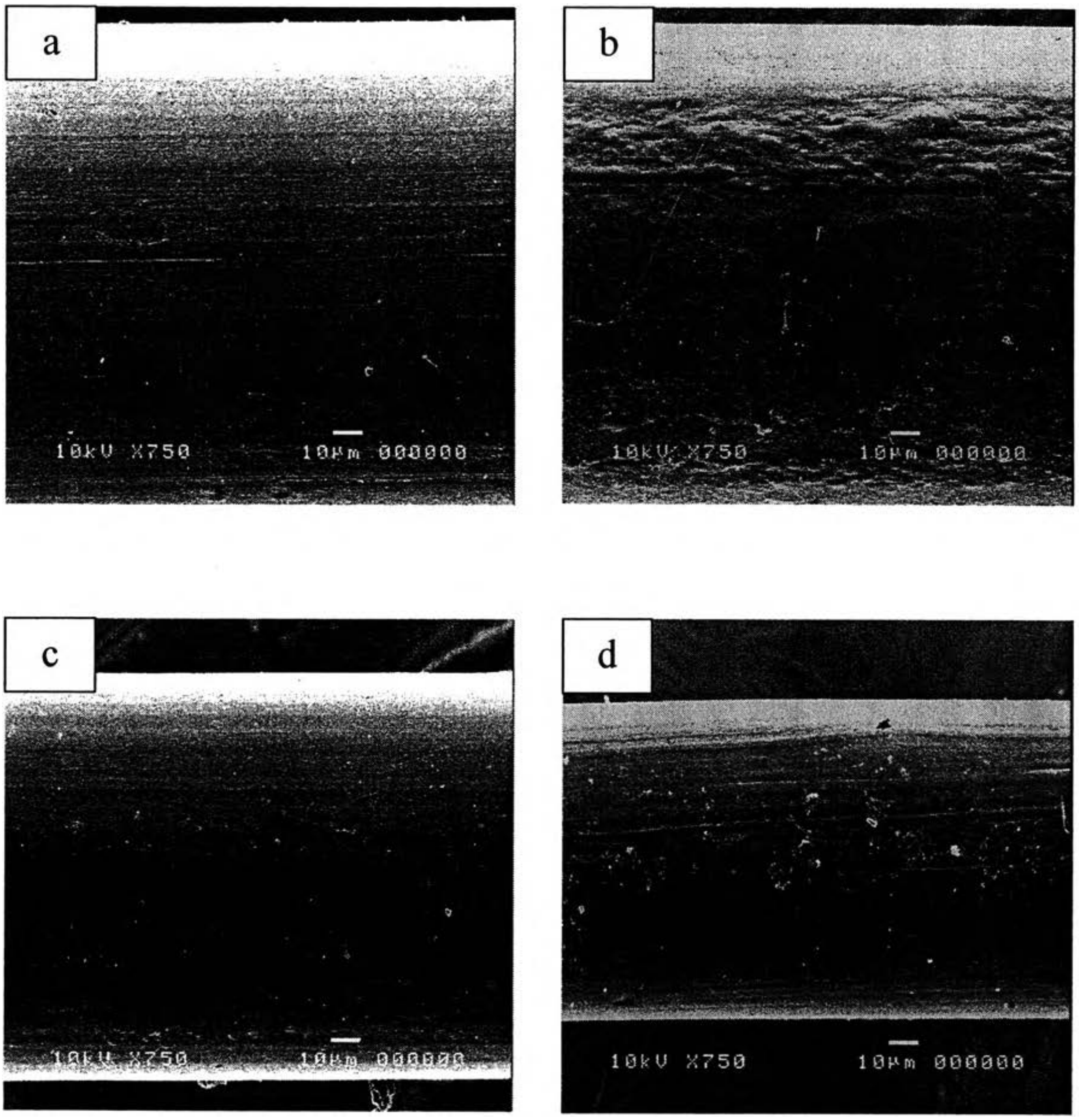

Figure 4.14 SEM images magnitude of 750 of PDLLA/PHBV/PEG1000/silver nanoparticles fibers (a) neat PDLLA/PHBV/PEG100 fibers (b–d). The addition of silver nitrate contents by weight are 0.2 (b), 0.3 (c) and 0.4 wt. % (d), respectively.

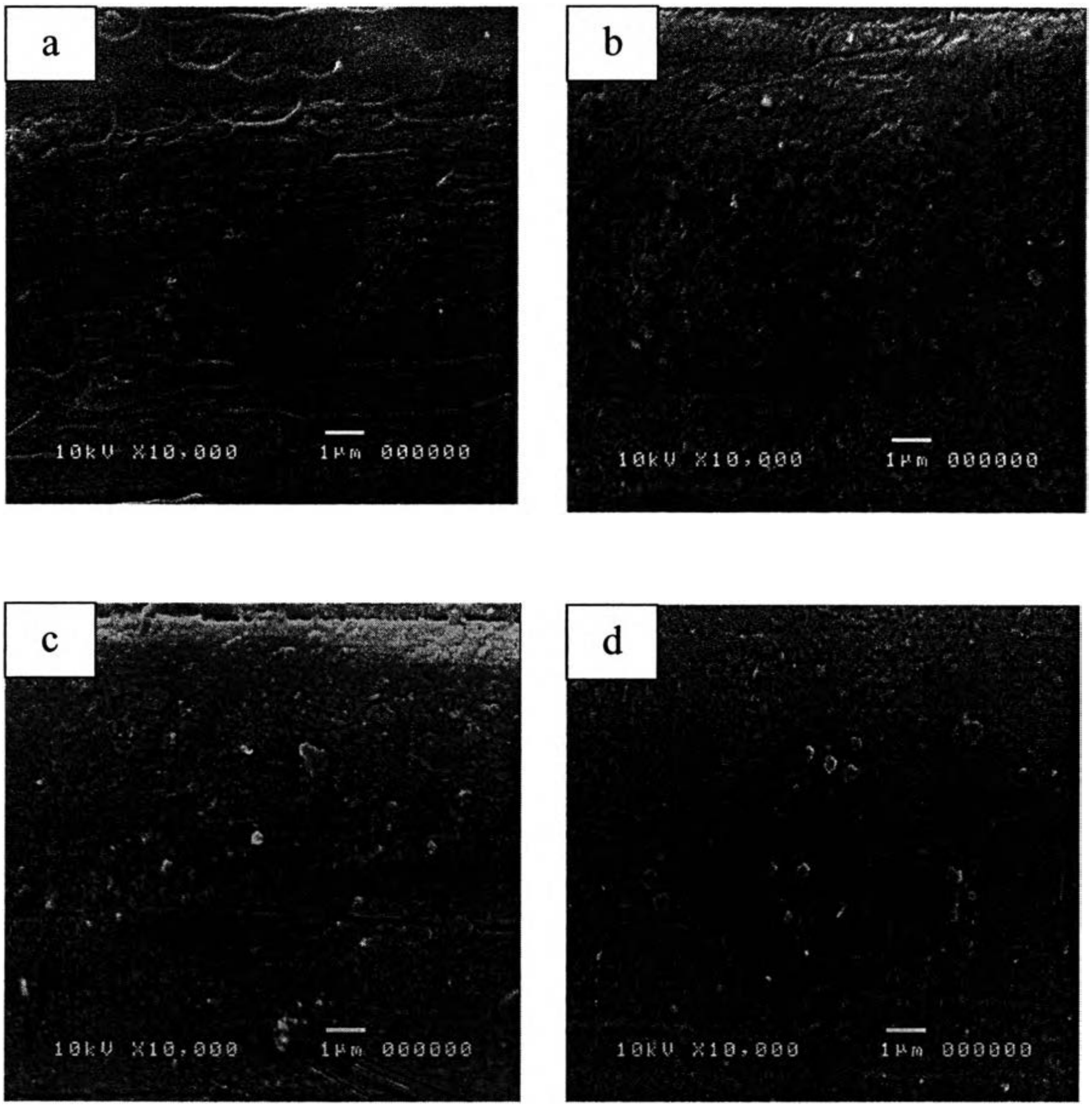

Figure 4.15 SEM images at magnitude of 10,000 of PDLLA/PHBV/PEG1000/silver nanoparticles fibers (a) neat PDLLA/PHBV/PEG100 fibers (b–d). The addition of silver nitrate contents by weight are 0.2 (b), 0.3 (c) and 0.4 wt. % (d), respectively.

4.4.3.3 Silver Ions Release

The in vitro silver ion release concentration of fiber containing silver nanoparticle were carried out in 5 mL of 0.02 mol L^{-1} phosphate buffered saline (PBS, pH= 7.4) and they were measured every 24 hours over 18-day test period by an atomic absorption spectrometer (AAs). As shown in Figure 4.16, the release of silver ion is relatively fast at the beginning of the test and becomes slower along the incubation time and the release can last more than 18 days.

In the study of the amount of released silver nanoparticle comparing with the total amount of silver nanoparticle in fiber is showed in Table 4.6. They show that silver nanoparticle can be released along 18 days from blending fiber only about 35% when comparing with the total amount of silver nanoparticle in fiber.

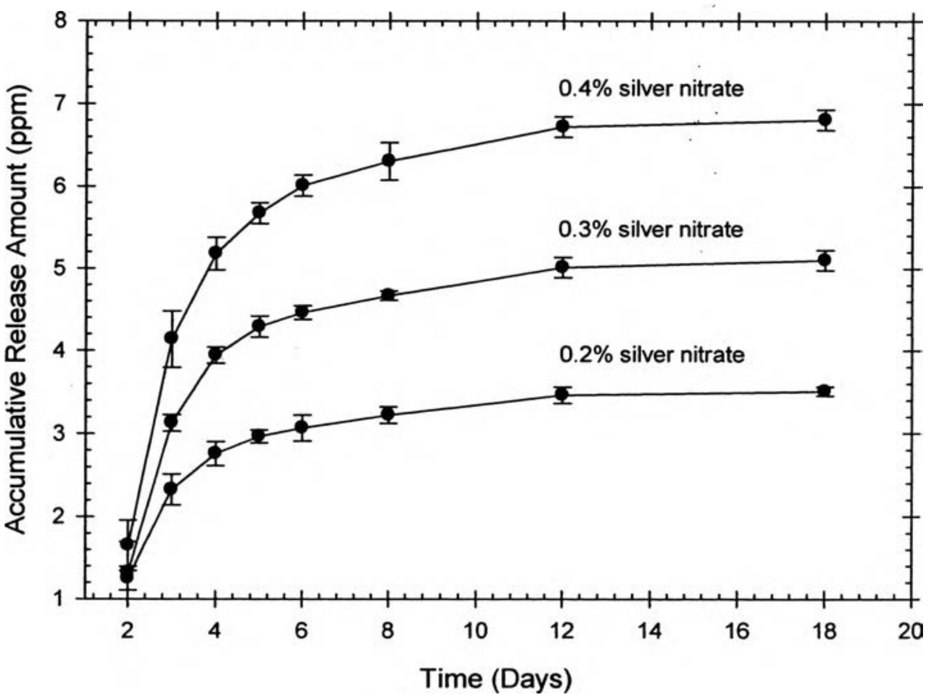

Figure 4.16 Silver ion release curves in PBS (pH = 7.4) at various silver ion content.

Table 4.6 The amount of released silver nanoparticle comparing with the total among of silver nanoparticle in fiber

Percentage of silver nitrate of blending fiber	Total among of silver nanoparticle in fiber (mg)	The among of released silver nanoparticle (mg)	Percentage of released silver nanoparticle (%)
0.2 % Silver nitrate	0.051±0.0006	0.017±0.0005	34.35±1.542
0.3 % Silver nitrate	0.076±0.0012	0.027±0.002	35.67±2.183
0.4 % Silver nitrate	0.101±0.0006	0.036±0.0006	35.20±0.817

4.4.3.4 Antibacterial activity

Antibacterial activity of PDLLA/PHBV/PEG1000 fiber containing silver nanopartcles was investigated s against S. aureus (Gram-positive) and E. coli (Gram-negative). Figure 4.17 demonstrates The US Clinical and Laboratory Standards Institute (CLSI) disc diffusion method was used to assess the antibacterial activity of these fibers. The result shows that the clear zone was found to increase with increasing silver nanoparticles and it was found to be more effective in sustain and reducing E. coli.

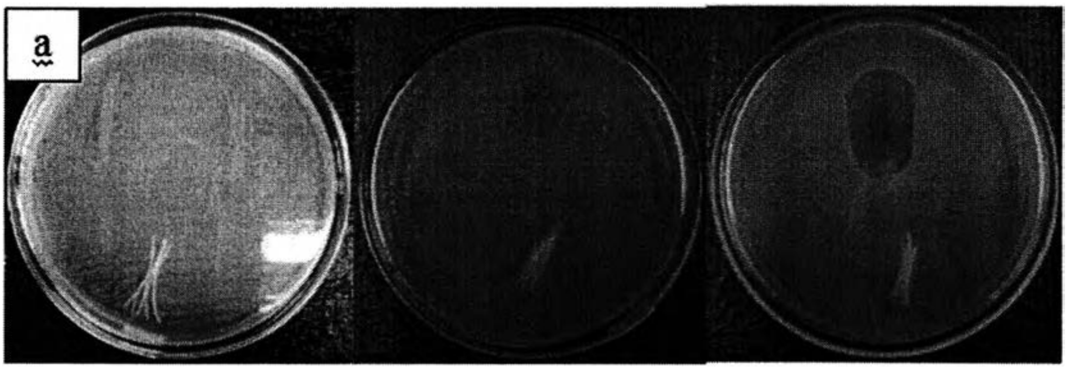

0.2% 0.3% 0.4%

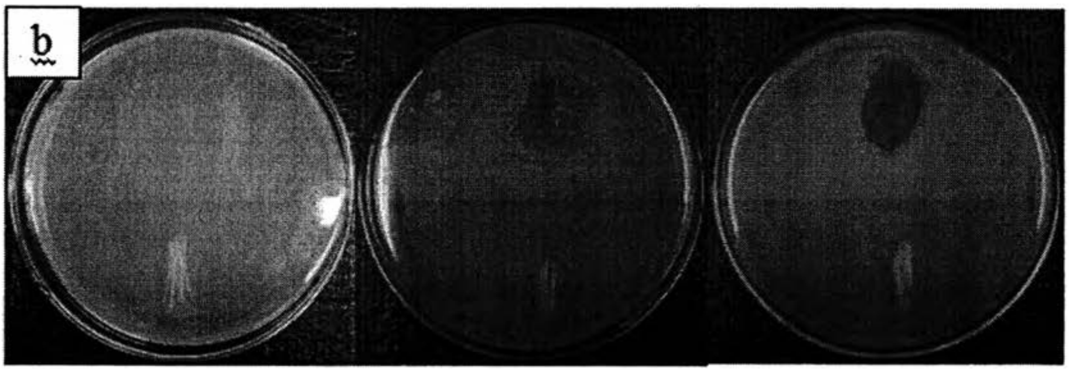

0.2% 0.3% 0.4%

Figure 4.17 Disc diffusion method for the assessment of the antibacterial activity of PDLLA/PHBV/PEG1000 containing various silver nanoparticles content against a) S. aureus and E. coli.

4.5 Conclusion

Poly(d,l-lactide) (PDLLA) was blended with Poly[(*R*)-3-hydroxybutyrate-*co*-(*R*)-3-hydroxyvalerate] (PHBV), poly(ethylene glycol) (PEG1000) and $AgNO_3$ to produce polymer blends containing antibacterial function. The suitable composition of polymer blends before adding $AgNO_3$ is 50PDLLA/50PHBV and 30% PEG1000 w/w of PDLLA/PHBV.These blends were spun into fiber by melt-spinning technique.

The PDLLA/PHBV blends are immiscible while the blending of 50PDLLA/50PHBV/PEG1000 is miscible as evidenced by a single, composition-dependent of T_g, T_{cc} and T_m of each polymer. Moreover, only the T_c of PHBV slightly increased when increasing silver nanoparticles content. For TGA data, Neat PDLLA was more thermally stable than neat PHBV. The addition of PEG1000 caused a shift of the onset temperature to a lower temperature while the addition of silver nanoparticles content caused a higher T_d of this blend.

Finally, the addition of PHBV and PEG1000 caused an increase in elongation at break from 3.7% for PDLLA to 413.8% for PDLLA/PHBV/PEG1000 while the addition of silver nanoparticles reduced this property. The antibacterial results showed that it can sustain and reduce E. coli and S. aureus and can release Ag ion for more than 18 days.

4.6 References

Brozl, M.E., VanderHart, D.L., Washburn, N.R. Biomaterials 2003;24:4181–4190.

Chen, L.,Wang, H., Wang, J., Chen, M., Shang, L. Journal of Biomedical Materials Research Part B: Applied Biomaterials. 2007;83: 589–595.

Couchman, P.R, Karasz, F.E. Macromolecules. 1978;11:117.

Furuhashi, Y., Imamurab, Y., Jikiharab, Y., Yamane, H. Polymer 2004;45: 5703–5712.

Fei, B., Chen, C., Wu, H., Peng, S., Wang, X., Dong., L. European Polymer Journal. 2003;39:1939–1946.

Fox, T.G., Bull. American Physical Society. 1956;2:123.

Gordon M, Taylor J.S. Journal Application Chemistry.1952;2:493.

Im, J.N., Kim, J.K., Kim, H.K., In, C.H., Lee K.Y., Park, W.H. Polymer Degradation and Stability. 2007;92:667-674

Ke, Z. B., Zheng, Z. F., Zhu, H. Y., Zhang, L. x., Gao, X. P. Desalination. 2009;236:1-7.

Kulinski, Z., Piorkowska E. Polymer. 2005;46:10290–10300

Liu, X., Dever, M., Fair, N., Benson, R.S. Journal of Environmental Polymer Degradation. 1997;5:225-235

Luo, C., Zhang, Y., Zeng, X., Zeng, Y., Wang, Y. Journal Colloidal Interface Science. 2005;288:444

Mi, F.L., Shyu, S.S., Linc, Y.M., Wuc, Y.B., Peng, C.K., Tsai, Y.H. Biomaterials. 2003;24:5023–5036.

Muriel, S., Jean, C., Michel, V. Polymer Degradation and Stability. 2006;91:2853–9.

Parra, D.F., Fusaro, J., Gaboardi, F., Rosa, D.S., Polymer Degradation and Stability 2006;91:1954–9.

Penning, J.P., Dijkstra, H., Pennings, A.J. Polymer. 1993;34:942–951.

Pillin, I., Montrelay, N., Grohens, Y. Polymer. 2006;47:4676–4682

Sondi, I., Salopek-Sondi, B. Journal of Colloid and Interface Science. 2004;275:177–182.

Wang, C.C, Su, C.H., Chen, J.P., Chen, C.C. Materials Science and Engineering. 2009

Wang, S., Ma, P., Wang, R., Wang, S., Zhang Y., Zhang, Y. Polymer Degradation and Stability. 2008;93:1364-1369

Tsuji, H, Ikada, Y. Macromol Chem Phys. 1996;197:3483.

Utracki, L.A. Advance Polymer Technology. 1985;5:33.

Xu, X., Yang, Q., Wang Y., Yu, H., Chen, X., Jing, X. European Polymer Journal. 2006;42:2081–2087.

Yang, D. S., Park, S.K., Neale, W.K. Composite Structures. 2009;88:497-508.

Zafar, F., Ashraf, S.M., Ahmad, S. Reactive & Functional Polymers 2007;67:928–935.